Effect of biochar on water migration to improve acidified soil

Jikai Lu (lujikai1996@163.com)
OUC: Ocean University of China
Yina Luo
Ocean University of China
Junlin Huang
Ocean University of China
Bingyan Hou
Ocean University of China
Bing Wang
Tokyo University of Agriculture and Technology: Tokyo Noko Daigaku
Kenji Ogino
Tokyo University of Agriculture and Technology: Tokyo Noko Daigaku
Jian Zhao
Ocean University of China

Research Article

Keywords: Application of biochar, Acidified soil improvement, Soil hydrological characteristic parameters, Molded soil

Posted Date: March 16th, 2022

DOI: https://doi.org/10.21203/rs.3.rs-1451104/v1

Effect of biochar on water migration to improve acidified soil

Jikai Lu[1,2] ·Yina Luo[1] ·Junlin Huang[1] ·Bingyan Hou[1] ·Bing Wang[3] ·Kenji Ogino[3] ·Jian Zhao[1]

Abstract

With the intensification of human activities, soil acidification has become a very serious threat to crop yield and food security. From a practical application perspective, this study used biochar to improve acidified soil. The concept of molded soil was put forward to examine the soil improvement effect of biochar. The changes in soil hydrological parameters suggested that biochar application improved the structure of acidified soil. The volumetric water content and vertical permeability coefficient of soil were improved to different degrees. In addition to increased soil moisture content due to biochar adsorption of soil micro-aggregates, biochar application improved the oxidation stability of soil organic carbon and promoted the formation of water-stable macro-aggregates. The molded soil showed little difference with acidified soil and was found representative and suitable for indoor small-scale regular exploratory experiments. This study found that leaching may promote the migration of acidic ions enhancing the biochar improvement efficiency of acidified soil, however, the phenomenon needs further study. This study provides theoretical support for acidified soil water retention, fertilizer conservation, obstacle elimination, productivity improvement of farmland, and reduction of groundwater non-point source pollution.

Keywords Application of biochar· Acidified soil improvement· Soil hydrological characteristic parameters· Molded soil

Introduction

Statistical data suggest the presence of nearly 3.95 billion square kilometers of acidified soil worldwide, accounting for nearly 30% of the non-glacier total land. Globally, nearly 2.5 billion square kilometers of cultivated land and potentially arable land are under the influence of soil acidification, accounting for almost 50% of the total cultivated land (Jin et al., 2020). Studies suggest that the number of microorganisms, bio-carbon, and nitrogen content in acidified soil decrease by 14.7, 19.1, and 12.1% respectively. These changes accelerate the dissolution of heavy metals promoting heavy metal toxicity to crops. The characteristics such as high intensity, large area, and wide distribution have become a serious threat to crop yield and food security. The present traditional and marketed acidified soil improvers increase the content of basic ions in the soil reducing aluminum toxicity and acidity. Besides, their high-frequency application gives rise to inevitable side effects (Mohammadi & Vanclooster, 2011). To solve the problem of soil acidification, experts and scholars have turned their attention to biochar (Fidel, Laird, & Spokas, 2018).

Soil bulk density refers to the weight of soil per unit volume in a natural state, which affects the soil permeability. Biochar with sufficient pore structure has a large specific surface area. The soil porosity

Jian Zhao
zhaojian@ouc.edu.cn
[1] College of Engineering, Ocean University of China, 239 Song-ling Road, Qingdao 266100, Shandong, China
[2] Energy Research Institute of Shandong Academy of Sciences, 19 Ke-yuan Road, Jinan 250014, Shandong, China
[3] Graduate School of Bio-Applications and Systems Engineering, Tokyo University of Agriculture and Technology, Koganei, Tokyo, 184-8588, Japan

can be improved after the continuous application of biochar reducing soil bulk density by adsorbing tiny soil aggregate particles. The soil with low bulk density and high organic matter content is more conducive to nutrient release, maintenance, and reduction (Chintala et al., 2014; Guszek, Guszek, Sas-Paszt, Sumorok, & Kozera, 2019). Also, it benefits seed germination saving the planting cost. Water content is an important factor of the soil environment that mainly depends on soil texture and local precipitation rate. Studies show that biochar can effectively improve the soil water holding capacity, however, in a limited range. Biochar is a renewable resource that can replace fossil raw materials as a green soil conditioner improving soil properties (Ahmad et al., 2016).

Many factors influence the improvement process of acidified soil, which limits the accurate analysis of biochar mechanism and improvement effect. This study utilized the concept of molded soil from uncultivated deep soil in mountainous areas, which was artificially acidified after high-temperature sterilization. Removal of humus, plant roots, inactivate microorganisms, and other factors can amplify the utility of biochar easing the analysis of acidified soil improvement effect (Guo et al., 2019). This study also examined whether the molded soil can be representative of acidified soil sampled from the field to obtain an improved scheme with high universality. This study provides theoretical support for improving the biochar effect reducing groundwater non-point source pollution (Moradi, Rasouli-Sadaghiani, Sepehr, Khodaverdiloo, & Barin, 2019; Oliveira et al., 2017). Also, the fields of environmental protection, crop production and protection, and cascade utilization of biomass resources can benefit from these findings (Lu et al., 2020).

1. Experimental materials and methods

1.1 Soils and biochar

This study used bio-carbon from peanut shell (BC) that was purchased from Shandong Huanba Environmental Protection and Energy Saving Equipment Technology Company. The basic physical and chemical properties of biochar are listed in Table. 1, and the scanning electron microscope (SEM) image is shown in Fig. 1. The molded soil was collected from uncultivated soil from the deep layer of Huai'an City, Jiangsu Province (118.54, 33.01). The acid soil (AS) was sampled from Qingdao City, Shandong Province (120.01, 36.28). The collected soil was naturally air-dried after removing impurities and screened with a 2 mm sieve. The soil moisture content was measured by a moisture meter (METTLER V10S) and the soil was stored for later use. Diluted concentrated hydrochloric acid (analytical grade) and deionized water, converted into 20% water content, were sprayed into the experimental molded soil. The process was repeated many times, each time pH change was within 0.05, to finally obtain the acidified molded soil (MS). The basic physical and chemical properties of the two kinds of soil samples are listed in
Table. 2.

Table. 1. Basic physical and chemical properties of biochar

	C_{ar} (%)	H_{ar} (%)	O_{ar} (%)	N_{ar} (%)	S_{ar} (%)	pH	Specific surface area (m^2/g)
BC	53.36	1.33	3.02	0.87	0.20	8.76	30.1180

Ar: as-received basis

Table. 2.Basic physical and chemical properties of sample soils

	pH	Volume weight of soil (g/cm^3)	Porosity (%)	Electrical conductivity (μS/cm)	Classification of soils
MS	5.20	1.38	48.54	206	Sandy loam
AS	5.23	1.32	49.36	624	Sandy loam

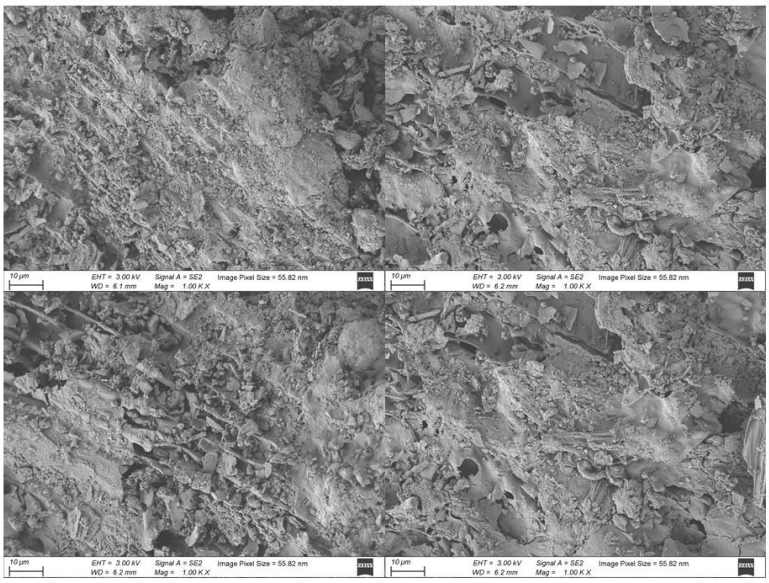

Fig. 1. SEM images of peanut shell biochar

1.2 Column model

The simulated soil-column container was a PVC plastic pipe with a height of 40 cm and a diameter of 10 cm. Five sampling holes with a diameter of 10 mm were opened at intervals of 5 cm from the top to the bottom. The bottom was sealed with the same material, and four leachate sampling holes with a diameter of 5 mm were opened on the circumference of 6 cm. Before usage, the soil-column container was repeatedly washed with 1 mol/L hydrochloric acid solution and deionized water. Also, Vaseline was evenly coated on the inner wall to prevent water from sticking to the wall and infiltration reducing the edge effect. The soil-column model is shown in Fig. 2.

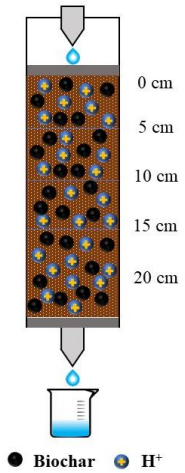

Fig. 2. The schematic diagram of the soil-column model

1.3 Experiment and sampling

The two acidified soil samples were air-dried and ground before mixing with 2 mm sieved BC. In total, five treatment groups were set up: treatment 1, the control group with no biochar (MS CK, AS CK); treatments 2 (MS 2%, AS 2%), 3 (MS 5%, AS 5%), 4 (MS 8%, AS 8%), and 5 (MS 10%, AS 10%) were one kilogram of soil sample mixed with 20, 50, 80, and 100 g of peanut shell biochar, respectively. Each treatment was replicated three times.

Bulk density and porosity were determined by evenly applying petroleum jelly to the inner wall of the ring knife, of which, the mass was weighed. Using a standard hand-held compaction apparatus, CK was uniformly loaded into the ring knife in two parts according to the set capacity of 1.38 g/cm^3. The other treatment groups were also operated similarly. The mass of each treatment was measured and the corresponding index was calculated according to equations (1) and (2).

$$\text{Bulk density}=\frac{m_1-m_0}{V} \tag{1}$$

$$\text{Porosity}=\left(1-\frac{\text{Bulk density}}{\rho}\right)\times 100\% \tag{2}$$

In the formula：m_0 denotes the weight of ring knife (g), m_1 denotes the weight of the ring knife after filling (g), V denotes the volume of the ring knife (cm^3), ρ denotes the soil density (g/cm^3).

Soil moisture characteristic curves: The soil samples from different treatment groups, in separate layers and uniformly packed in a ring knife, were saturated with water for 24 h. Soil moisture characteristic curves were obtained using a pressure film meter. Different suction forces were applied at 0.02, 0.04, 0.06, 0.08, 0.10, 0.50, 0.80, 1.0, 3.0, 5.0, 7.0, 10.0, and 12.0 bar and the weight of each sample was recorded after reaching equilibrium. Then the samples were placed at 105°C and dried to a constant weight. The obtained data were used to plot the soil moisture characteristics curve.

Vertical infiltration of soil water: The experimental equipment consisted of a 10 cm wide and 40 cm high soil column, and a 6 cm wide and 60 cm high Martens bottle. Soil samples from each treatment group were uniformly filled into the column in 4 batches, and water was continuously supplied to the column using the marsupial. The vertical infiltration and infiltrating rate of the soil in each treatment group were measured within 120 minutes and the curve was plotted with the obtained data.

1.4 Data processing and analysis

The experimental data were summarized and plotted by Excel 2019 and Origin 2017, linearly fitted by MATLAB 2018 and Origin 2017, and analyzed by SPSS 25.0 statistical software using one-way ANOVA between and within groups, respectively. The significance level was set to 0.05.

2. Results and analysis

2.1 Effect of biochar on soil bulk density and porosity

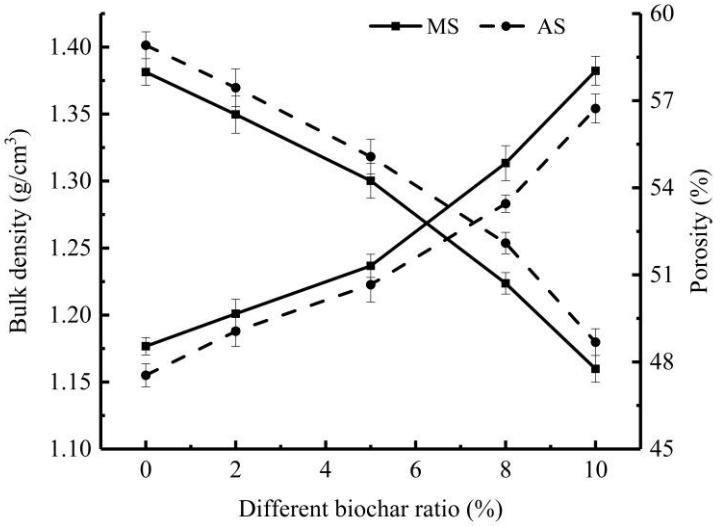

Fig. 3.Change in soil bulk density and soil porosity under different carbon blending ratio

Soil bulk density directly correlates to the soil conditions (Ola, Gauthier, Xiong, & Lovelock, 2019). Change in soil bulk density generally means a change in the soil structure affecting soil porosity. The changes in soil bulk density and porosity of the two soil samples mixed with biochar with different carbon-soil ratios are shown in Fig. 3. Compared with the control group, soil bulk density of AS decreased by 2.26, 5.94, 10.54, and 15.81%, and soil porosity increased by 3.19, 6.56, 12.43, and 19.33% respectively. Soil bulk density of MS decreased by 2.29, 5.88, 11.41, and 16.04%, and soil porosity increased by 2.31, 5.71, 12.99, and 19.55% respectively, showing significant differences among the treatment groups ($p<0.05$). The increase of biochar application in acid soil gradually decreased the soil bulk density and increased soil porosity. This can be attributed to the formation of pore structure by volatile organic components in biochar during pyrolysis and carbonization (Zhang et al., 2019). Biochar, with a better pore structure and large specific surface area, adsorbs tiny soil aggregate particles reducing soil bulk density and increasing porosity. This change improves the exchange of soil moisture and gas (Boostani, Najafi-Ghiri, & Hardie, 2020). Notably, the 10% treatment group showed the most prominent effect with MS soil bulk density of 1.15g/cm^3 and soil porosity of 58.03%; the AS soil bulk density was 1.18g/cm^3 with soil porosity of 56.73%. Compared with AS, MS showed lower soil bulk density and higher soil porosity, which mainly depends on the soil characteristics before improvement.

2.2 Effect of biochar on soil moisture

Soil moisture characteristic curves are used to study soil hydrodynamics. MATLAB was applied to achieve curve fitting between experimental results of 10 treatment groups using the Van Genuchren model.

$$\theta = \theta_r + \frac{\theta_s - \theta_r}{[1+(\alpha P)^n]^m} \tag{3}$$

In the formula：θ denotes the volume moisture content of acidified soil (cm^3/cm^3). P denotes soil water suction (par). θ_s and θ_r are the saturated water content and residual water content of acid soil, respectively (cm^3/cm^3). α, m, and n are parameters from Van Genuchren model.

As shown in equations (3), "m=1-1/n" was selected for curve fitting, "α", "n", and correlation coefficient R^2 are shown in Table. 3. R^2 in different treatment groups was >0.92 indicating the validity of experimental data. The soil moisture characteristic curves under different carbon ratios are shown in Fig. 4.

Table. 3.Parameters of Van Genuchren model of acidified soil under different carbon blending ratios

Treatment groups	Parameters of Van Genuchren model		
	α	n	R^2
MS CK	0.0223	1.4383	0.9857
MS 2%	0.0220	1.4419	0.9526
MS 5%	0.0219	1.4398	0.9447
MS 8%	0.0215	1.4305	0.9567
MS 10%	0.0211	1.4407	0.9325
AS CK	0.0217	1.4158	0.9876
AS 2%	0.0213	1.4264	0.9523
AS 5%	0.0208	1.4193	0.9412
AS 8%	0.0204	1.4359	0.9551
AS 10%	0.0201	1.4225	0.9294

As shown in Fig. 4, the overall volume water content in the MS group was slightly higher than in the AS group but the difference was not significant ($p>0.05$). However, the overall trend of change in soil moisture characteristics under different treatments was the same. Specifically, in the range of 0-1 bar soil water suction, the soil moisture content dropped rapidly; a higher carbon ratio led to a slower drop in water content. After that, with the increase of soil water suction, the soil-water characteristic curve became stable. Under the same soil suction condition, the soil volume water content among different treatments increased with the increase in carbon ratio showing a trend of CK <2% <5% <8% <10%. The average moisture content of MS 2%, MS 5%, MS 8%, and MS 10% was 1.4, 1.7, 2.0, and 2.1 times as that of MS CK. Likewise, the average moisture content of AS 2%, AS 5%, AS 8%, and AS 10% was 1.4, 1.7, 2.0, and 2.2 times as that of AS CK showing significant differences among the treatment groups ($p<0.05$). With the increase of pressure, the soil moisture content in the respective treatment group was generally higher than that of the control group. In the range of 0.02-0.06 bar, the average soil moisture content of MS 2% and AS 2% treatment groups increased by 17.83% and 18.74% compared with their respective control groups. In the range of 0.08-3.0 bar, these increased by 64.28% and 65.74%, and in the range of 5.0~12.0 bar, the increase was by 81.60 and 88.25%, respectively. These results showed that

under the same soil water suction pressure, the addition of biochar to the soil effectively increased the soil water content indicating the good water-holding characteristics of biochar. With the increase in soil water suction, the biochar treatment group always remained better than the control group. This can be attributed to the physical structure of biochar. Rich pore structure and high specific surface area of biochar strongly improve soil adsorption inhibiting water loss that effectively maintains the soil moisture (Sorrenti, Masiello, Dugan, & Toselli, 2016).

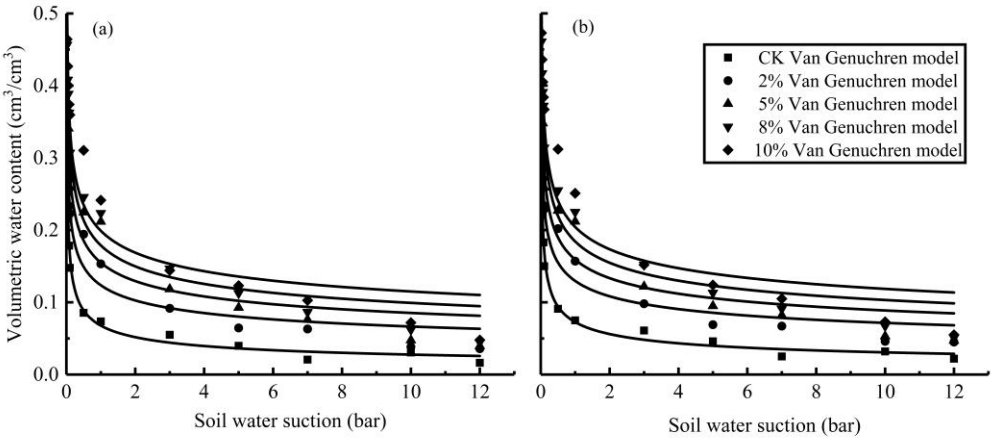

Fig. 4. Soil moisture characteristic curves under different carbon ratios
(a) MS; (b) AS

2.3 Effect of biochar on vertical infiltration of soil

The vertical infiltration of acidified soil water is an important part of water circulation and transfer (Su et al., 2018). The data for vertical infiltration rate and infiltration time of acidified soil were fitted with the Kostiakov infiltration model by Origin software, as in equations (4); the correlation coefficient of the fitting is 0.9438. The cumulative infiltration amount and infiltration time showed a quadratic polynomial relationship, and the equations (5) was fitted by Origin software with an average correlation coefficient of 0.9668. This indicated the credibility of experimental results shown in Table. 4.

$$K_i = kt^a \quad (4)$$

$$W_t = At^2 + Bt + C \quad (5)$$

In these formulas, K_i denotes the infiltration of the acidified soil (mm/min). k represents the infiltration coefficient of acidified soil (mm/min). a denotes the infiltration index of acidified soil. W_t is the cumulative infiltration amount of acidified soil (cm); t is the infiltration time (min). A, B, and C are empirical constants of the Kostiakov infiltration model.

The data chart of vertical water infiltration rate of acidified soil with infiltration time is shown in Fig. 5. It can be seen that the changing trend of each treatment is almost the same. In the first 10 min of infiltration time, the infiltration rate dropped rapidly and then decreased slowly until became stable. In

the end, both soil samples showed that a higher carbon ratio led to a lower infiltration rate, that is, 10% <8% <5% <2% <CK. MS showed a decrease by 42.62, 38.25, 31.69, and 26.23%, and AS showed a decrease by 41.35, 38.07, 30.21, and 26.69% showing significant differences between groups ($p<0.05$). Compared with AS, the overall soil vertical infiltration rate was lower for MS; the proportion of decrease in infiltration rate after adding biochar was more prominent.

Table. 4. Water vertical permeability parameters of acidified soil at any time under different carbon ratios

Treatment	Kostiakov infiltrating model			Quadratic polynomial			
groups	k	a	R^2	A	B	C	R^2
MS CK	14.7098	-0.5737	0.9398	-0.00306	0.6977	6.0791	0.9736
MS 2%	11.5382	-0.5983	0.9407	-0.00125	0.2967	5.0695	0.9532
MS 5%	10.2477	-0.5924	0.9397	-0.00094	0.2161	3.7561	0.9544
MS 8%	9.3776	-0.5734	0.9385	-0.00038	0.1347	3.0310	0.9526
MS 10%	8.5931	-0.5662	0.9411	-0.00042	0.1288	2.0787	0.9629
AS CK	15.0793	-0.5470	0.9576	-0.00309	0.7187	5.5358	0.9871
AS 2%	9.0597	-0.5697	0.9472	-0.00128	0.3133	4.6392	0.9699
AS 5%	5.5730	-0.4202	0.9464	-0.00099	0.2284	3.4376	0.9676
AS 8%	3.4544	-0.2928	0.9332	-0.00042	0.1445	2.7771	0.9672
AS 10%	2.4123	-0.2075	0.9538	-0.00041	0.1357	1.9016	0.9799

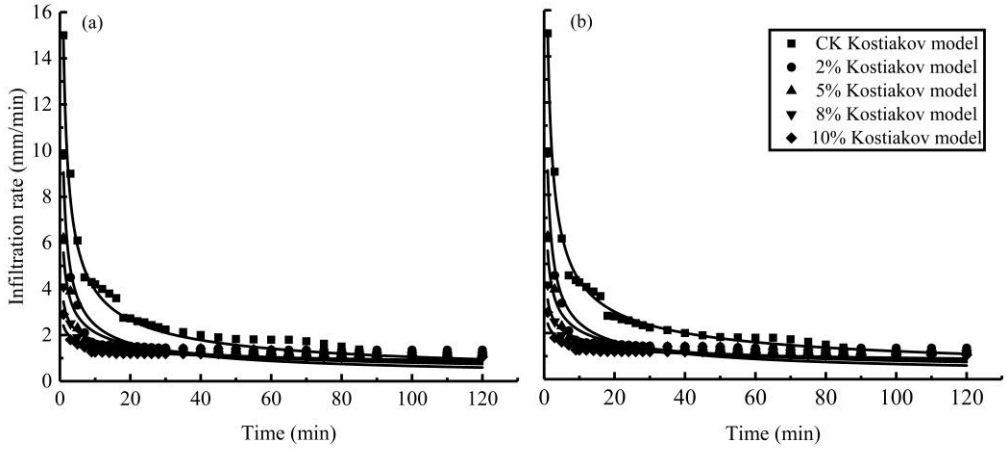

Fig. 5. Effect of biochar on vertical infiltration rate of soil under different carbon mixing ratios (a) MS; (b) AS

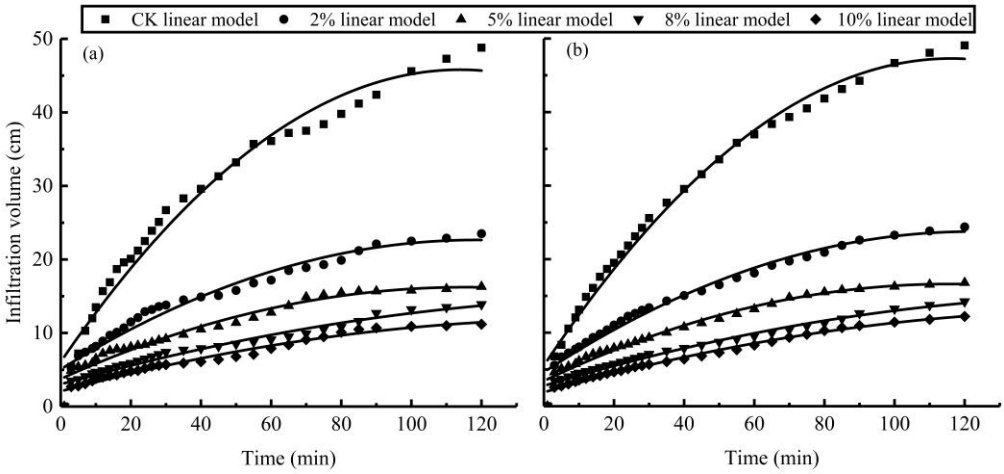

Fig. 6. Effect of biochar on vertical infiltration of soil under different carbon ratios
(a) MS; (b) AS

The change in vertical infiltration of soil with infiltration time is shown in Fig. 6. With the extension of infiltration time, the vertical infiltration of acid soil increased continuously. The increase was inversely proportional to the amount of biochar. At the end of the infiltration experiment, the vertical infiltration of MS 2%, MS 5%, MS 8% and MS 10% was 48.15, 33.40, 28.48 and 22.95% of MS CK, and that of AS 2%, AS 5%, AS 8% and AS 10% was 49.69 and 49.69% of AS CK ($p<0.05$). Biochar addition remarkably improved the vertical infiltration rate and infiltration rate of the soil. It seems that biochar reduced the vertical infiltration rate and infiltration rate of soil by increasing the soil water content. This is consistent with the water characteristic curve of soil showing great potential for water and fertilizer retention. Barrios also confirmed through experiments that a higher carbon content increases this effect (Barrios et al., 2019). Meanwhile, considering the soil bulk density, porosity, volume water content, vertical infiltration rate, and infiltration amount, the influence of biochar on MS characteristics was obvious and representative of filed soil, suggesting MS suitability for indoor small-scale exploratory experiments.

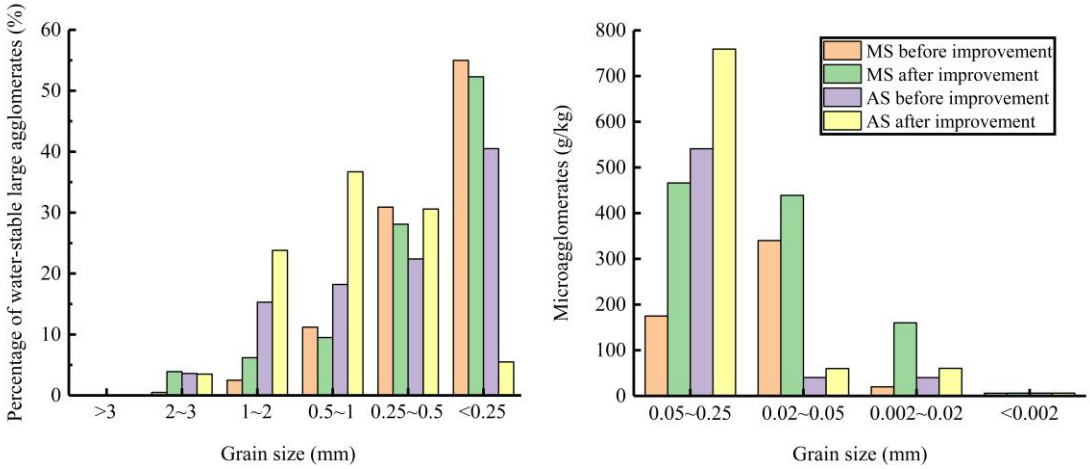

Fig. 7. Change in the proportion of water-stable macroaggregates before and after biochar addition

To explore the influence of biochar addition on the structure of acidified soil water holding capacity, two kinds of soils before and after improvement for the 10% treatment groups were collected to compare the changes in soil aggregates. Soil aggregation plays important role in soil's ability to retain water and

fertilizer. On the one hand, biochar improves the stability of soil aggregates because of its porous structure and large specific surface area promoting large aggregates. On the other hand, it increases the organic matter content of acidified soil; organic carbon, a good soil binder, promotes soil aggregation (Shah et al., 2017). To investigate the effect of biochar on acidified soil aggregation, the 10% treatment groups were selected for showing the best improvement effect. The changes in the contents of water-stable aggregates and microaggregates are shown in Fig. 7. Before the biochar addition, the large water-stable aggregates were mostly in small size (<0.5 mm); MS and AS accounted for 85.9 and 62.9% of the total aggregates. The micro-aggregates were mostly large in size (0.05-0.25 mm); 175 and 541g/kg in MS and AS, respectively. Biochar mixing into the two soils made the obvious structural change to the soil after improvement. The proportion of water-stable macroaggregates with particle size >1 mm increased by 7.1% in MS. In AS, water-stable macroaggregates with particle size >0.25 mm increased by 35%. The content of microaggregates with different particle sizes increased in both soils, with an overall increase of 332 and 218 g/kg, respectively. This change enhanced the soil water adsorption capacity improving the water-holding capacity. In general, micro-aggregation affects the physical properties of the soil improving microbial proliferation, ion fixation, and nutrient release.

3. Conclusions

The application of biochar into acidified soil effectively improved its internal structure increasing water-holding capacity, reducing non-point source pollution, and slowing the release of fertilizer. These results lay a foundation for further research on the influence of biochar on ion migration in acid soil under leaching state.

Biochar mixing into acidified soil improved soil bulk density and porosity. With the increase of biochar application amount, the soil bulk density gradually decreased and soil porosity gradually increased showing a positive correlation with biochar amount. Compared with MS, AS showed higher soil bulk density and lower soil porosity due to its inherent characteristics. Biochar promoted soil micro-aggregation which affected the porosity and bulk density of AS. Furthermore, soil moisture characteristic curves showed that in the low range soil water suction, the water content of AS dropped rapidly, and then the curve became stable at soil water suction >1 bar. A higher carbon ratio led to higher soil moisture. Under the same soil water suction, there was no obvious difference between MS and AS; the average soil water content increased by 1.4-2.2 times compared with the respective control groups. The rich oxygen-containing functional groups, strong hydrophilicity, and high specific surface area of biochar provide it good water-holding capacity improving the acidified soil-water environment. The experiments showed that with the extension of infiltration time, the vertical infiltration rate and infiltration amount decreased in AS with the increase in biochar amount. Also, biochar increased water-stable macro-aggregates >1 mm in MS by 7.1%, and >0.25 mm in AS by 35%. The content of microaggregates with different particle sizes in the two soils increased by 332 and 218 g/kg, respectively. Organic carbon acted as the soil binder. Moreover, we found that prepared MS showed only a little difference to AS and is suitable for indoor small-scale regular exploratory experiments.

Acknowledgements

Thanks are due to the Energy Research Institute of Shandong Academy of Sciences for providing experimental equipment. And thanks to all the reviewers who participated in the review, as well as MJEditor (www.mjeditor.com) for providing English editing services during the preparation of this manuscript.

Author contribution Jikai Lu: conceptualization, data curation, formal analysis, methodology, writing, visualization and editing. Yina Luo: conceptualization, writing and editing. Junlin Huang: Investigation, editing, and method development. Bing Wang and Kenji Ogino: method development and paper review. Jian Zhao: editing, general supervision, and funding acquisition. Bingyan Hou: conceptualization, general supervision, and funding acquisition. All authors read and approved the final version to be published.

Funding This study was supported by Key R&D Program of Shandong Province (Major Innovation Project)(No.2021CXGC010803)

Declarations

Ethics approval and consent to participate Not applicable.
Consent for publication Not applicable.
Competing interests The authors declare no competing interests.

References

Ahmad, M., Lee, S. S., Lee, S. E., Al-Wabel, M. I., Tsang, D. C. W., & Ok, Y. S. (2016). Biochar-induced changes in soil properties affected immobilization/mobilization of metals/metalloids in contaminated soils. *Journal of Soils and Sediments, 17*(3), 717-730.https://doi.org/10.1007/s11368-015-1339-4

Barrios, R. E., Gaonkar, O., Snow, D., Li, Y., Li, X., & Bartelt-Hunt, S. L. (2019). Enhanced biodegradation of atrazine at high infiltration rates in agricultural soils. *Environ Sci Process Impacts, 21*(6), 999-1010. Retrieved from https://www.ncbi.nlm.nih.gov/pubmed/31115391. https://doi.org/10.1039/c8em00594j

Boostani, H. R., Najafi-Ghiri, M., & Hardie, A. G. (2020). Evaluation of nickel stabilization in a calcareous soil amended with biochars using mathematical adsorption models. *Communications in Soil Science and Plant Analysis, 51*(9), 1213-1226. https://doi.org/10.1080/00103624.2020.1763382

Chintala, R., Schumacher, T. E., Mcdonald, L. M., Clay, D. E., Malo, D. D., Papiernik, S. K., . . . Julson, J. L. (2014). Phosphorus Sorption and Availability from Biochars and Soil/Biochar Mixtures. *CLEAN - Soil, Air, Water, 42*(5), 626-634. https://doi.org/10.1002/clen.201300089

Fidel, R. B., Laird, D. A., & Spokas, K. A. (2018). Sorption of ammonium and nitrate to biochars is electrostatic and pH-dependent. *Sci Rep, 8*(1), 17627. Retrieved from https://www.ncbi.nlm.nih.gov/pubmed/30514956. https://doi.org/10.1038/s41598-018-35534-w

Guo, S., Gao, Y., Wang, Y., Liu, Z., Wei, X., Peng, P., . . . Yang, Y. (2019). Urea/ZnCl2 in situ hydrothermal carbonization of Camellia sinensis waste to prepare N-doped biochar for heavy metal removal. *Environ Sci Pollut Res Int, 26*(29), 30365-30373. Retrieved from https://www.ncbi.nlm.nih.gov/pubmed/31435909. https://doi.org/10.1007/s11356-019-06194-8

Guszek, S., Guszek, S., Sas-Paszt, L., Sumorok, B., & Kozera, R. (2019). Biochar-rhizosphere interactions -a review. https://doi.org/10.5604/01.3001.0010.6288

Jin, L., Wei, D., Yin, D., Zhou, B., Ding, J., Wang, W., . . . Wang, L. (2020). Investigations of the effect of the amount of biochar on soil porosity and aggregation and crop yields on fertilized black soil in northern China. *PLoS One, 15*(11), e0238883.

https://doi.org/10.1371/journal.pone.0238883

Lu, J., Yang, Y., Liu, P., Li, Y., Huang, F., Zeng, L., . . . Hou, B. (2020). Iron-montmorillonite treated corn straw biochar: Interfacial chemical behavior and stability. *Science of the Total Environment, 708*(C).https://doi.org/10.1016/j.scitotenv.2019.134773

Mohammadi, M. H., & Vanclooster, M. (2011). Predicting the Soil Moisture Characteristic Curve from Particle Size Distribution with a Simple Conceptual Model. *Vadose Zone Journal, 10*(2), 594-602. https://doi.org/https://doi.org/10.1016/j.scitotenv.2019.134773

Moradi, S., Rasouli-Sadaghiani, M. H., Sepehr, E., Khodaverdiloo, H., & Barin, M. (2019). Soil nutrients status affected by simple and enriched biochar application under salinity conditions. *Environmental Monitoring & Assessment, 191*(4).https://doi.org/10.1007/s10661-019-7393-4

Ola, A., Gauthier, A. R. G., Xiong, Y., & Lovelock, C. E. (2019). The roots of blue carbon: responses of mangrove stilt roots to variation in soil bulk density. *Biol Lett, 15*(4), 20180866. https://doi.org/10.1098/rsbl.2018.0866

Oliveira, F. R., Patel, A. K., Jaisi, D. P., Adhikari, S., Lu, H., & Khanal, S. K. (2017). Environmental application of biochar: Current status and perspectives. *Bioresour Technol, 246*, 110-122. https://doi.org/10.1016/j.biortech.2017.08.122

Shah, A. N., Tanveer, M., Shahzad, B., Yang, G., Fahad, S., Ali, S., . . . Souliyanonh, B. (2017). Soil compaction effects on soil health and cropproductivity: an overview. *Environ Sci Pollut Res Int, 24*(11), 10056-10067. https://doi.org/10.1007/s11356-017-8421-y

Sorrenti, G., Masiello, C. A., Dugan, B., & Toselli, M. (2016). Biochar physico-chemical properties as affected by environmental exposure. *Sci Total Environ, 563-564*, 237-246. https://doi.org/doi:10.1016/j.scitotenv.2016.03.245

Su, L., Yang, X., Wang, Q., Qin, X., Zhou, B., & Shan, Y. (2018). Functional Extremum Solution and Parameter Estimation for One-Dimensional Vertical Infiltration using the Brooks-Corey Model. *Soil Science Society of America Journal, 82*(6), 1319-1332. https://doi.org/10.2136/sssaj2018.01.0016

Zhang, X., Dou, S., Ndzelu, B. S., Guan, X. W., Zhang, B. Y., & Bai, Y. (2019). Effects of different corn straw amendments on humus composition and structural characteristics of humic acid in black soil. *Communications in Soil Science and Plant Analysis, 51*(1), 107-117. https://doi.org/10.1080/00103624.2019.1695827